

# Co(II) and Ni(II) Complexes with Imidazole-Containing Ligands: Synthesis, Structural Characterization, and Magnetic Property<sup>1</sup>

H. W. Kuai\*, X. C. Cheng, D. Y. Jiang, T. Hu, D. H. Li, and X. H. Zhu

Faculty of Chemical Engineering, Huaiyin Institute of Technology, Huai'an, 223003 P.R. China

\*e-mail: hyitshy@126.com

Received April 28, 2015

**Abstract**—Hydrothermal reaction of Co(II) salt with 1,4-di(1-imidazolyl)benzene ( $L^1$ ) and 4,4'-oxydipthalic acid ( $H_4OA$ ) yields a new complex  $[\text{Co}_3(\text{HOA})_2(L^1)_4(\text{H}_2\text{O})_4]$  (**I**).  $[\text{Ni}(L^2)_2\text{SO}_4] \cdot 0.5\text{H}_2\text{O}$  (**II**) can be obtained via the hydrothermal reaction of  $\text{NiSO}_4 \cdot 6\text{H}_2\text{O}$  with 1,3-di(1*H*-imidazol-4-yl)benzene ( $L^2$ ). Complexes **I** and **II** have been characterized by single-crystal and powder X-ray diffraction (CIF files CCDC nos. 1019291 (**I**) and 1019292 (**II**)), IR, elemental, and thermogravimetric analyses. Complex **I** exhibits the uninodal six-connected 3D **pcu** framework structure of **I** with  $(4^{12} \cdot 6^3)$  topology; Complex **II** consists of the uninodal four-connected 2D **sql** ( $4^4 \cdot 6^2$ ) networks. In addition, magnetic property of **I** was investigated.

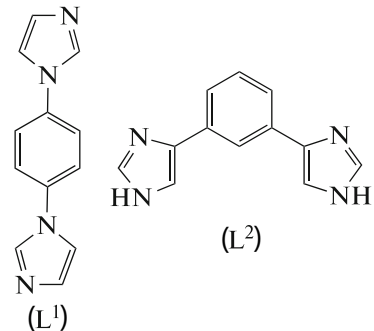
**DOI:** 10.1134/S1070328416020044

## INTRODUCTION

In recent years, the rational design and assembly of coordination polymers is rapidly growing in coordination, materials and supramolecular chemistry due to their fascinating structures and their potential applications in many fields [1, 2]. Currently, the exploration of new crystalline materials has become the uppermost aim of crystal engineering. It is known that functional properties of complexes are largely dependent on their architectures and the nature of the metal centers and of the bridging ligands, which provide a feasibility to pursue diversification of functional properties of complexes via achievement of structural diversity. However, the self-assembly process of complexes is rather complicated and is subtly influenced by many factors such as the coordination geometry of the metal centers, connection modes of organic ligands as well as the synthetic conditions [3, 4]. According to previous studies, the intrinsic nature of organic ligands has been proven to play a decisive role in directing the final structure and properties [5, 6].

Generally, the multidentate organic ligands containing coordination sites of N and/or O donors are always regarded as excellent candidates for the construction of desirable frameworks [7, 8]. Among them, imidazole-containing ligands such as 1,4-di(1-imidazolyl)benzene ( $L^1$ ), 1,3-di(1*H*-imidazol-4-yl)benzene ( $L^2$ ), and 1,3,5-tris(1-imidazolyl)benzene have been widely utilized in the formation of complexes [9–11]. On the other hand, the polycarboxylates such as benzenedicarboxylate and benzenetricarboxylate

also deserve more attention for their versatile coordination modes, structural diversity, and thermodynamic stability [12, 13]. Recent studies further demonstrated that mixed organic ligands, especially the mixed N-donor and O-donor, are excellent blocks for the construction of novel complexes for the existence of more tunable factors [14–16]. Following such synthetic strategy, we focus our attention in this study on coordination reactions of  $L^1$  and  $L^2$  in the presence of different O-donor ligands with metal salts:



We aim at seeking for new complexes with fascinating structures and interesting properties. We report herein the syntheses and characterization of two new complexes  $[\text{Co}_3(\text{HOA})_2(L^1)_4(\text{H}_2\text{O})_4]$  (**I**) and  $[\text{Ni}(L^2)_2\text{SO}_4] \cdot 0.5\text{H}_2\text{O}$  (**II**), which were obtained under different synthetic conditions.

## EXPERIMENTAL

**Materials and methods.** All commercially available chemicals are of reagent grade and were used as

<sup>1</sup> The article is published in the original.

received without further purification. The  $L^1$  and  $L^2$  ligands were synthesized via the experimental procedure as reported in the literature [9, 10]. Elemental analysis of C, H, and N were taken on a Perkin-Elmer 240C elemental analyzer. Infrared spectra (IR) were recorded on a Bruker Vector22 FT-IR spectrophotometer by using KBr pellets. Thermogravimetric analysis (TGA) was performed on a simultaneous SDT 2960 thermal analyzer under nitrogen atmosphere with a heating rate of  $10^\circ\text{C min}^{-1}$ . Powder X-ray diffraction (PXRD) patterns were measured on a Shimadzu XRD-6000 X-ray diffractometer with  $\text{Cu}K_\alpha$  ( $\lambda = 1.5418 \text{ \AA}$ ) radiation at room temperature. The magnetic measurement in the temperature range of 1.8 to 300 K was carried out on a Quantum Design MPMS7 SQUID magnetometer in a field of 2000 Oe.

**Synthesis of I.** The mixture of  $\text{Co}(\text{NO}_3)_2 \cdot 6\text{H}_2\text{O}$  (58.2 mg, 0.2 mmol),  $\text{H}_4\text{OA}$  (34.6 mg, 0.1 mmol), and  $L^1$  (42.0 mg, 0.2 mmol) in 10 mL DMF– $\text{H}_2\text{O}$  (1 : 1,  $V/V$ ) was sealed in a 16 mL Teflon-lined stainless-steel container and heated at  $140^\circ\text{C}$  for 72 h. Then the oven was cooled down at a rate of  $10^\circ\text{C/h}$ . After cooling to room temperature, pale brown block crystals of I were obtained with an approximate yield of 30% based on the  $L^1$ .

For  $\text{C}_{80}\text{H}_{62}\text{N}_{16}\text{O}_{22}\text{Co}_3$  ( $M = 1776.24$ )

anal. calcd., %: C, 54.09; H, 3.52; N, 12.62.  
Found, %: C, 54.32; H, 3.71; N, 12.85.

IR data ( $\nu$ ,  $\text{cm}^{-1}$ ): 1690  $\nu(\text{C=O})$ , 1612  $\nu_{as}(\text{COO}^-)$ , 1547  $\nu_{as}(\text{COO}^-)$ , 1428  $\nu_s(\text{COO}^-)$ , 1386  $\nu_s(\text{COO}^-)$ .

**Synthesis of II.** The mixture of  $\text{NiSO}_4 \cdot 6\text{H}_2\text{O}$  (26.2 mg, 0.1 mmol) and  $L^2$  (42.0 mg, 0.2 mmol) in 10 mL DMF– $\text{H}_2\text{O}$  (1 : 1,  $V/V$ ) was sealed in a 16 mL Teflon-lined stainless-steel container and heated at  $120^\circ\text{C}$  for 48 h. Then the oven was shut off and cooled down naturally at ambient temperature. After cooling to room temperature, green block crystals of II were obtained with an approximate yield of 45% based on the  $L^2$ .

For  $\text{C}_{48}\text{H}_{42}\text{N}_{16}\text{O}_9\text{S}_2\text{Ni}_2$  ( $M = 1168.47$ )

anal. calcd., %: C, 49.34; H, 3.62; N, 19.18.  
Found, %: C, 49.12; H, 3.85; N, 19.33.

IR data ( $\nu$ ,  $\text{cm}^{-1}$ ): 3447  $\nu(\text{NH})$ , 1654  $\nu(\text{C=N})$ .

**X-ray structure determinations.** The crystallographic data collections for complexes I, II were carried out on a Bruker Smart ApexII CCD area-detector diffractometer using graphite-monochromated  $\text{Mo}K_\alpha$  radiation ( $\lambda = 0.71073 \text{ \AA}$ ) at 293(2) K. The diffraction data were integrated by using the SAINT program [17], which was also used for the intensity corrections for the Lorentz and polarization effects. Semi-empirical absorption correction was applied using the

SADABS program [18]. The structures of I, II were solved by direct methods and all non-hydrogen atoms were refined anisotropically on  $F^2$  by the full-matrix least-squares technique using the SHELXL-97 crystallographic software package [19]. In I, II, all hydrogen atoms in C atoms were generated geometrically. The hydrogen atoms in O atoms in I could be found at reasonable positions in the difference Fourier maps and located there, while the hydrogen atoms of lattice water in II could not be located and thus were not included in the refinement. The details of crystal parameters, data collection, and refinements for the complexes are summarized in Table 1; the selected bond lengths and angles are listed in Table 2.

Supplementary material has been deposited with the Cambridge Crystallographic Data Centre (nos. 1019291 (I) and 1019292 (II); deposit@ccdc.cam.ac.uk or <http://www.ccdc.cam.ac.uk>).

## RESULTS AND DISCUSSION

The hydrothermal reaction of  $\text{Co}(\text{NO}_3)_2 \cdot 6\text{H}_2\text{O}$  with the  $L^1$  and  $\text{H}_4\text{OA}$  at  $140^\circ\text{C}$  leads to the formation of complex I; when the  $L^2$  reacts with  $\text{NiSO}_4 \cdot 6\text{H}_2\text{O}$  under the hydrothermal condition at  $120^\circ\text{C}$ , complex II can be obtained. Complexes I and II are stable in air.

X-ray structural analysis has shown that complex I consists of 3D frameworks. The asymmetric unit of I contains one Co(II) atom, one centrosymmetric Co(II), one  $\text{HOA}^{3-}$  ligand, one  $L^1$ , two halves of  $L^1$ , and two coordinated water molecule (Fig. 1a). Each cobalt cation is six-coordinated and exhibits octahedral coordination geometry ( $[\text{CoN}_2\text{O}_4]$  for Co(1) and  $[\text{CoN}_3\text{O}_3]$  for Co(2)). The bond distances around cobalt cations are in the range from 2.108(2) to 2.130(2)  $\text{\AA}$  for Co(1) and from 2.047(2) to 2.182(2)  $\text{\AA}$  for Co(2). The  $\text{HOA}^{3-}$  ligand contains four carboxylate groups, but just two of them take part in coordination, and the rest are free. So the  $\text{HOA}^{3-}$  in I may look more like phthalate. One coordinated carboxylate adopts  $\mu_1\text{-}\eta^1\text{:}\eta^0$ -monodentate mode and the other is  $\mu_2\text{-}\eta^1\text{:}\eta^1$ -bridging one, two of which link three Co(II) atoms to form a secondary building unit (SBU)  $[\text{Co}_3(\text{COO})_2]$ . Adjacent SBUs are doubly bridged by  $L^1$  ligands to exhibit a chain structure (Fig. 1b). Then,  $L^1$  as two-connector rods can further bridge different chains to fabricate a 3D framework architecture (Fig. 1c). The topological analysis was carried out to get insight of the structure of I. As mentioned above, each SBU  $[\text{Co}_3(\text{COO})_2]$  is neighbored by eight  $L^1$  ligand; each  $L^1$  ligand as a two-connector will be simplified as a linear bridge. Because adjacent SBUs are doubly bridged by the linear  $\mu_2$ -bridges  $L^1$ , each SBU should not be viewed as a 8-connector node, but a six-connected one. Therefore, the resulting structure of I

**Table 1.** Crystallographic data and structure refinement details for complexes **I** and **II**

Parameter	Value	
	<b>I</b>	<b>II</b>
Crystal system	Triclinic	Triclinic
Space group	$P\bar{1}$	$P\bar{1}$
$a$ , Å	8.187(5)	9.8665(18)
$b$ , Å	12.549(5)	11.457(2)
$c$ , Å	17.765(5)	13.025(2)
$\alpha$ , deg	99.171(5)	65.029(3)
$\beta$ , deg	96.039(5)	83.497(3)
$\gamma$ , deg	92.988(5)	86.423(4)
$V$ , Å <sup>3</sup>	1787.4(14)	1326.0(4)
$Z$	1	1
$\rho_{\text{calcd}}$ , mg/m <sup>3</sup>	1.650	1.463
$F(000)$	911	602
$\theta$ Range, deg	1.65–25.01	1.73–28.00
Reflections collected	8957	11582
Independent reflections ( $R_{\text{int}}$ )	6190 (0.0148)	6273 (0.0313)
Reflections with $I > 2\sigma(I)$	5359	4872
Number of refinement parameters	547	350
Goodness-of-fit on $F^2$	1.038	1.061
$R_1$ ( $I > 2\sigma(I)$ )*	0.0400	0.0513
$wR_2$ ( $I > 2\sigma(I)$ )**	0.0945	0.1488
Largest diff. peak and hole, $e \text{ \AA}^{-3}$	0.498 and -0.553	1.191 and -0.446

\*  $R_1 = \sum \|F_o - |F_c\|/\sum |F_o\|$ . \*\*  $wR_2 = |\sum w(|F_o|^2 - |F_c|^2)|/\sum |w(F_o)|^2|^{1/2}$ , where  $w = 1/[\sigma^2(F_o^2) + (aP)^2 + bP]$ ,  $P = (F_o^2 + 2F_c^2)/3$ .

can be simplified as a uninodal six-connected 3D **pcu** framework with  $(4^{12} \cdot 6^3)$  topology (Fig. 1d) [20].

Complex **II** exhibits a 2D network structure based on the interconnection of Ni(II) and the L<sup>2</sup> ligand. There are one Ni(II), two L<sup>2</sup>, one SO<sub>4</sub><sup>2-</sup>, and half of lattice water in the asymmetrical unit. Each Ni<sup>2+</sup> cation is six-coordinated by four imidazole N atoms and two O atoms from SO<sub>4</sub><sup>2-</sup>, to furnish a distorted octahedral coordination geometry [NiN<sub>4</sub>O<sub>2</sub>] (Fig. 2a). The

bond distances around Ni(II) atom vary from 2.041(3) to 2.196(2) Å. Each L<sup>2</sup> ligand links two Ni(II) atoms, and each Ni(II) is surrounded by four L<sup>2</sup> ligands. This kind of connection proceeds infinitely to generate a 2D network structure (Fig. 2b). Using topology to analyze the structure, each Ni(II) can be regarded as a four-connector node and each two-connector L<sup>2</sup> ligand acts as a linear bridge. The resultant structure of **II** can be simplified as a uninodal four-connected 2D **sql** ( $4^4 \cdot 6^2$ ) network (Fig. 2c).

**Table 2.** Selected bond lengths (Å) and angles (deg) for complexes **I** and **II**<sup>\*</sup>

Bond	<i>d</i> , Å	Bond	<i>d</i> , Å
<b>I</b>			
Co(1)–O(1)	2.119(2)	Co(1)–O(10)	2.109(3)
Co(1)–N(1)	2.130(2)	Co(2)–O(2)	2.106(2)
Co(2)–O(3)	2.047(2)	Co(2)–O(11)	2.181(2)
Co(2)–N(5)	2.156(3)	Co(2)–N(7)	2.106(3)
Co(2)–N(4) <sup>#1</sup>	2.134(3)		
<b>II</b>			
Ni(1)–O(1)	2.187(2)	Ni(1)–O(2)	2.196(2)
Ni(1)–N(1)	2.066(3)	Ni(1)–N(5)	2.040(3)
Ni(1)–N(7) <sup>#1</sup>	2.046(3)	Ni(1)–N(3) <sup>#2</sup>	2.096(3)
Angle	$\omega$ , deg	Angle	$\omega$ , deg
<b>I</b>			
O(1)Co(1)O(10)	88.29(8)	O(1)Co(1)N(1)	97.03(8)
O(2)Co(2)O(3)	88.53(7)	O(10)Co(1)N(1)	88.42(9)
O(2)Co(2)N(5)	174.26(8)	O(2)Co(2)O(11)	88.62(7)
O(2)Co(2)N(4) <sup>#1</sup>	86.72(8)	O(2)Co(2)N(7)	87.34(8)
O(3)Co(2)N(5)	96.51(8)	O(3)Co(2)O(11)	176.62(8)
O(3)Co(2)N(4) <sup>#1</sup>	85.06(8)	O(3)Co(2)N(7)	92.34(9)
O(11)Co(2)N(7)	89.34(8)	O(11)Co(2)N(5)	86.25(8)
N(5)Co(2)N(7)	95.17(9)	O(11)Co(2)N(4) <sup>#1</sup>	92.97(8)
N(4) <sup>#1</sup> Co(2)N(7)	173.57(9)	N(4) <sup>#1</sup> Co(2)N(5)	90.97(9)
<b>II</b>			
O(1)Ni(1)O(2)	65.36(9)	O(1)Ni(1)N(1)	85.38(10)
O(1)Ni(1)N(5)	162.88(12)	O(1)Ni(1)N(7) <sup>#1</sup>	99.65(11)
O(1)Ni(1)N(3) <sup>#2</sup>	88.66(10)	O(2)Ni(1)N(1)	88.66(11)
O(2)Ni(1)N(5)	97.54(11)	O(2)Ni(1)N(7) <sup>#1</sup>	164.96(11)
O(2)Ni(1)N(3) <sup>#2</sup>	84.66(11)	N(1)Ni(1)N(5)	93.68(11)
N(1)Ni(1)N(7) <sup>#1</sup>	88.92(12)	N(1)Ni(1)N(3) <sup>#2</sup>	172.47(12)
N(5)Ni(1)N(7) <sup>#1</sup>	97.43(13)	N(3) <sup>#2</sup> Ni(1)N(5)	90.66(11)
N(3) <sup>#2</sup> Ni(1)N(7) <sup>#1</sup>	96.63(12)		

<sup>\*</sup> Symmetry transformations used to generate equivalent atoms: <sup>#1</sup>  $-x, 1-y, 2-z$  (**I**) and <sup>#1</sup>  $x, -1+y, z$ , <sup>#2</sup>  $x, 1+y, -1+z$  (**II**).

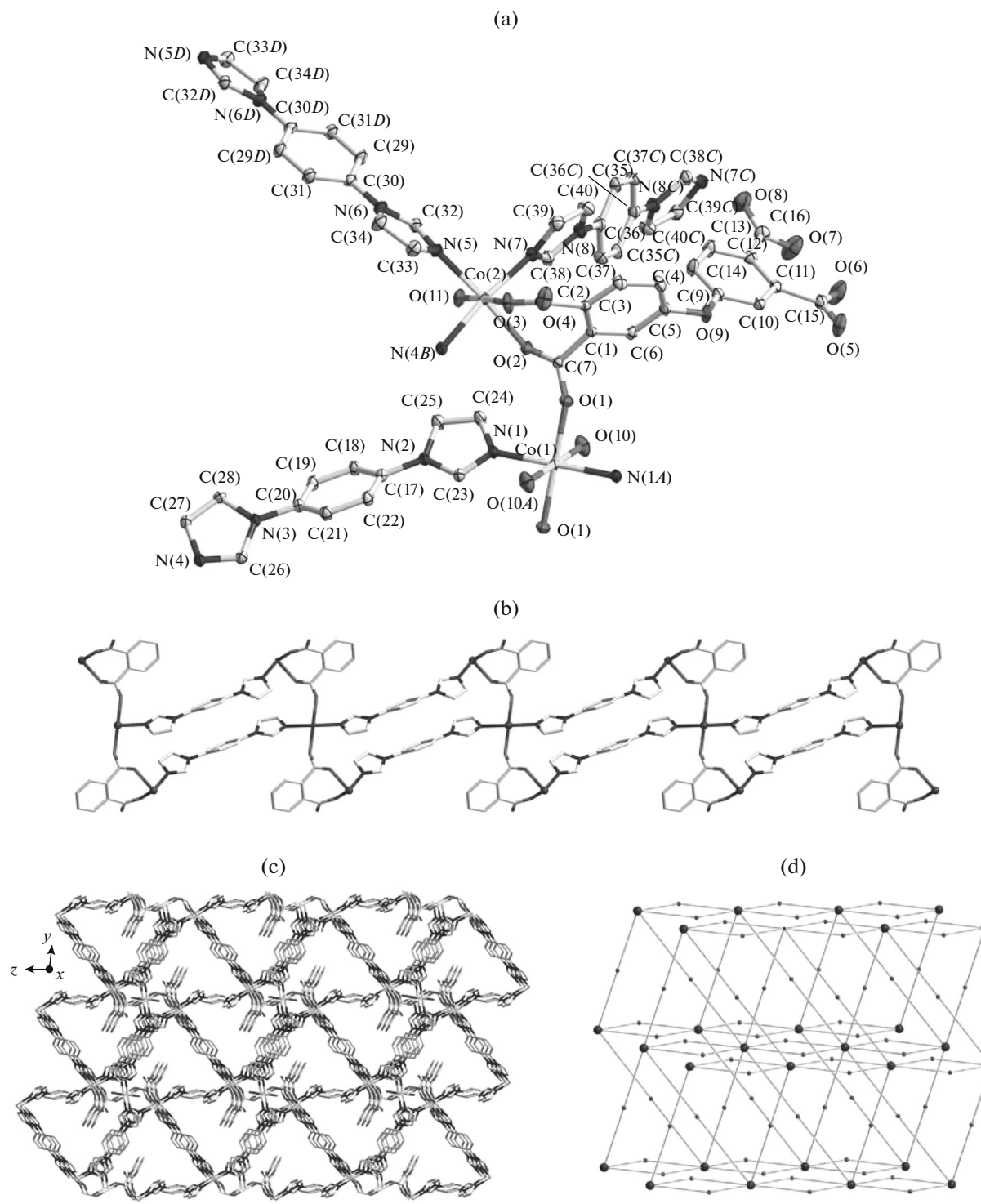


**Fig. 1.** The coordination environment of the  $\text{Co}^{2+}$  ions in **I** with ellipsoids drawn at the 30% probability level. The hydrogen atoms are omitted for clarity (a); view of the chain structure in **I** (b); view of the 3D architecture of **I** (c) (some organic moieties are omitted for clarity); view of the uninodal six-connected **pcu** framework of **I** with  $(4^{12} \cdot 6^3)$  topology (d).

The phase purity of **I**, **II** could be proved by PXRD analyses. Each pattern of the bulk sample was in agreement with the simulated pattern from the corresponding single crystal data.

TGA were carried out for complexes **I** and **II**, and the results of TGA are shown in Fig. 3. Complex **I** shows a weight loss (4.32%) in the temperature range of 130–180°C, corresponding to the loss of coordi-

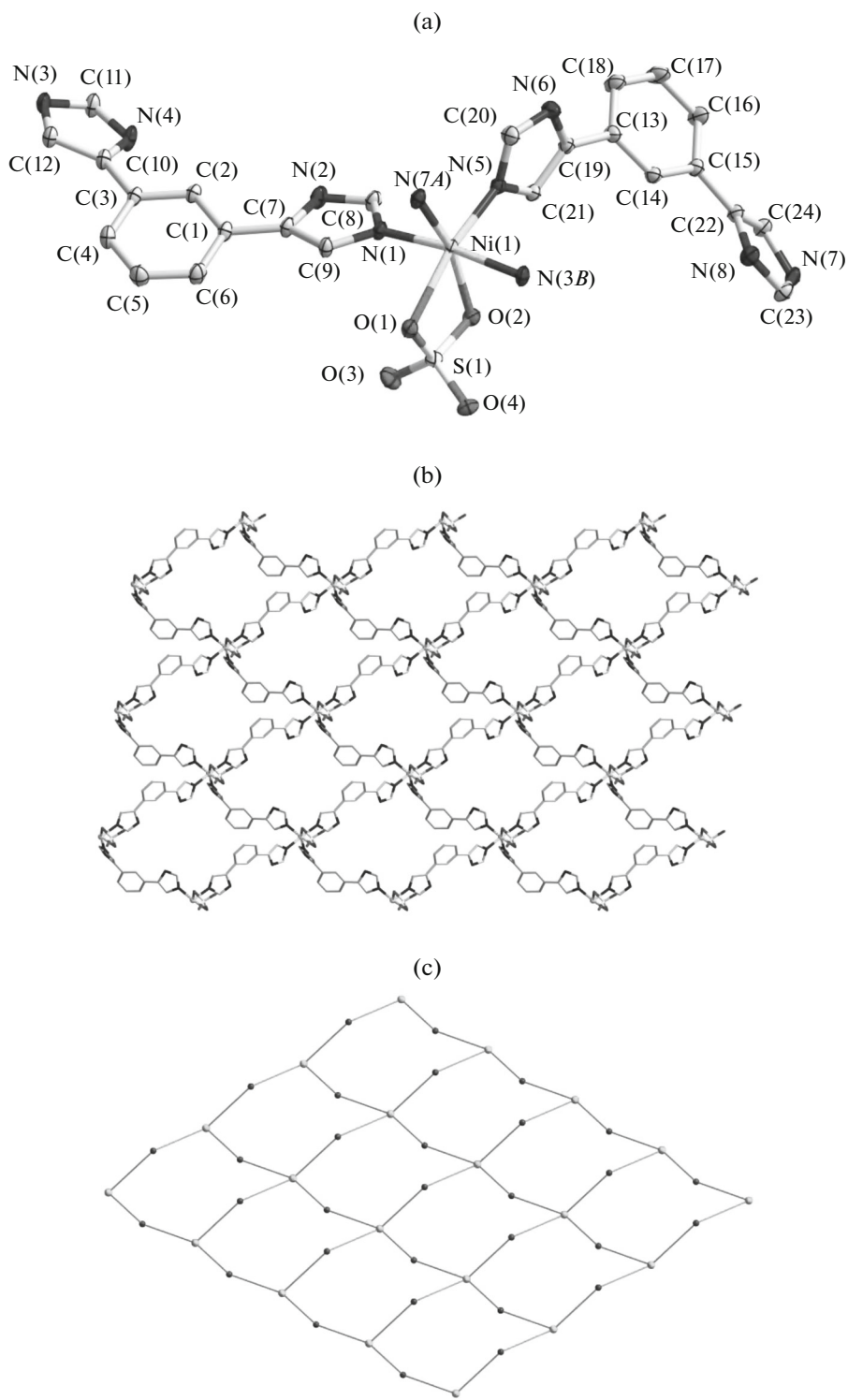


**Fig. 2.** The coordination environment of Ni ions in **II** with ellipsoids drawn at the 30% probability level (a) (the hydrogen atoms and lattice water are omitted for clarity); view of the 2D network of **II** (b); view of uninodal 3-connected **sql** network of **II** with  $(4^4 \cdot 6^2)$  topology (c).

nated water (calcd. 4.06%), and the residue is stable up to about 380°C. For complex **II**, there is a weight loss (1.26%) from 60–110°C, attributed to the release of lattice water (calcd. 1.54%), and the

decomposition of the residue can be observed at 290°C nearby.

The temperature dependence of magnetic susceptibility of **I** was investigated from 300 to 1.8 K with an

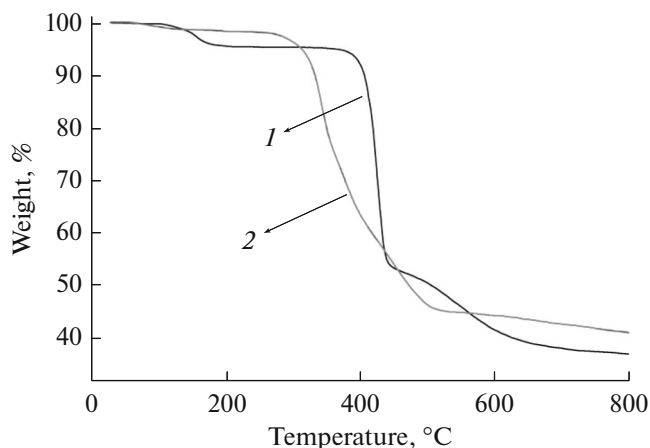


Fig. 3. The TGA curves of complexes of **I** (1) and **II** (2).

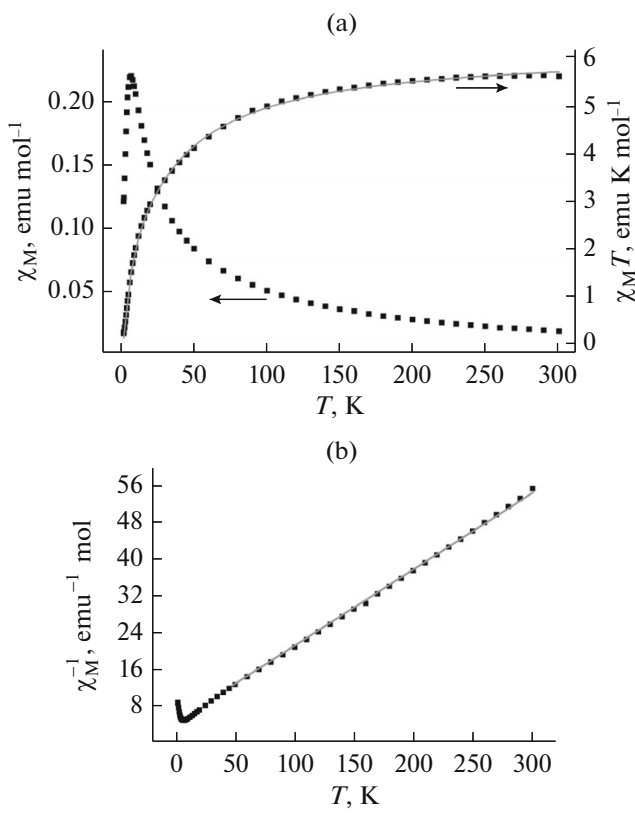


Fig. 4. Temperature dependences of magnetic susceptibility: of  $\chi_M$  and  $\chi_M T$  for **I** (a); of  $\chi_M^{-1}$  for **I** (b). The solid line represents the fitted curve.

applied magnetic field of 2000 Oe. The  $\chi_M$ ,  $\chi_M^{-1}$ , and  $\chi_M T$  vs.  $T$  curves for **I** are shown in Fig. 4. The value of  $\chi_M T$  at room temperature is  $5.68 \text{ cm}^3 \text{ K mol}^{-1}$ , which is larger than the expected spin-only value ( $5.62 \text{ cm}^3 \text{ K mol}^{-1}$ ) for three high-spin Co(II) centers ( $g = 2$  and

$s = 3/2$ ) [21]. The temperature dependence of  $\chi_M^{-1}$  above 50 K obeys the Curie–Weiss equation of  $\chi_M^{-1} = (T - \theta)/C$  with the Curie–Weiss constants:  $C = 6.12 \text{ cm}^3 \text{ mol}^{-1} \text{ K}$ ,  $\theta = -27.16 \text{ K}$ . The negative value of  $\theta$  and the shape of the  $\chi_M T$  vs.  $T$  curve suggest there may exist antiferromagnetic interactions between the neighboring Co(II) centers [22].

In order to estimate the strength of the magnetic interactions in **II**, the following equation was used [23]:  $\chi_M T = A \exp(-E_1/kT) + B \exp(-E_2/kT)$ . Here,  $A + B$  equals the curie constant ( $C$ ), and  $E_1$ ,  $E_2$  represent the “activation energies” corresponding to the spin-orbit coupling and the magnetic exchange interaction, respectively. The obtained values of  $A + B = 6.18 \text{ cm}^3 \text{ mol}^{-1} \text{ K}$  and  $E_1/k = 36.05 \text{ K}$  agree with those given in a previous report [23]. The value of  $-E_2/k = -4.36 \text{ K}$ , corresponding to  $J = -8.72 \text{ K}$ , further proved that the antiferromagnetic interactions exist between neighboring  $\text{Co}^{2+}$  ions in **I** [24].

#### ACKNOWLEDGMENTS

The authors gratefully acknowledge Huaian Administration of Science and Technology of Jiangsu Province of China (HAG2013019) for financial support of this work.

#### REFERENCES

1. Kuai, H.W., Cheng, X.C., and Zhu, X.H., *J. Coord. Chem.*, 2013, vol. 66, no. 1, p. 28.
2. Jia, J.M., Liu, S.J., Cui, Y., et al., *Cryst. Growth Des.*, 2013, vol. 13, no. 1, p. 4631.
3. Zhang, K.L., Hou, C.T., Song, J.J., et al., *CrystEngComm*, 2012, vol. 14, no. 2, p. 590.
4. Zhang, K.L., Chang, Y., Zhang, J.B., et al., *CrystEngComm*, 2012, vol. 14, no. 13, p. 2926.
5. Kuai, H.W., Cheng, X.C., and Zhu, X.H., *J. Coord. Chem.*, 2013, vol. 66, no. 11, p. 1795.
6. Kuai, H.W., Xu, X.Y., Cheng, X.C., et al., *J. Coord. Chem.*, 2013, vol. 66, no. 24, p. 4304.
7. Kuai, H.W., Cheng, X.C., and Zhu, X.H., *Polyhedron*, 2013, vol. 50, p. 390.
8. Kuai, H.W., Cheng, X.C., and Zhu, X.H., *Inorg. Chem. Commun.*, 2012, vol. 25, p. 43.
9. Chen, Z.H., Zhao, Y., Chen, S.S., et al., *J. Solid State Chem.*, 2013, vol. 202, p. 215.
10. Chu, Q., Su, Z., Fan, J., et al., *Cryst. Growth Des.*, 2011, vol. 11, no. 9, p. 3885.
11. Su, Z., Fan, J., Okamura, T.A., et al., *Cryst. Growth Des.*, 2010, vol. 10, no. 4, p. 1911.
12. Kuai, H.W., Cheng, X.C., and Zhu, X.H., *Polyhedron*, 2013, vol. 53, p. 113.
13. Su, Z., Chen, M., Okamura, T.A., et al., *Inorg. Chem.*, 2011, vol. 50, no. 3, p. 985.
14. Chen, S.S., Chen, M., Takamizawa, S., et al., *Chem. Commun.*, 2011, vol. 47, no. 17, p. 4902.

15. Kuai, H.W., Hou, C., and Sun, W.Y., *Polyhedron*, 2013, vol. 52, p. 1268.
16. Kuai, H.W., Cheng, X.C., Feng, L.D., et al., *Z. Anorg. Allg. Chem.*, 2013, vol. 639, nos. 12–13, p. 2337.
17. *SAINT, Program for Data Extraction and Reduction*, Madison: Bruker AXS, Inc., 2001.
18. Sheldrick, G.M., *SADABS, Program for Bruker Area Detector Absorption Correction*, Göttingen: Univ. of Göttingen, 1997.
19. Sheldrick, G.M., *SHELXS/L-97, Programs for the Determination of Crystal Structure*, Göttingen: Univ. of Göttingen, 1997.
20. Blatov, V.A., *TOPOS, a Multipurpose Crystalllochemical Analysis with the Program Package*, Samara State University, Russia, 2009.
21. Ghoshal, D., Mostafa, G., Maji, T.K., et al., *New J. Chem.*, 2004, vol. 28, no. 10, p. 1204.
22. Chen, M., Chen, S.S., Okamura, T.A., et al., *Cryst. Growth Des.*, 2011, vol. 11, no. 5, p. 1901.
23. Rueff, J.M., Masciocchi, N., Rabu, P., et al., *Chem. Eur. J.*, 2002, vol. 8, no. 8, p. 1813.
24. Herrera, J.M., Bleuzen, A., Dromzée, Y., et al., *Inorg. Chem.*, 2003, vol. 42, no. 22, p. 7052.